CrossMark

REVIEW

Lung morphometry: the link between structure and function

Ewald R. Weibel[1]

Abstract The study of the structural basis of gas exchange function in the lung depends on the availability of quantitative information that concerns the structures establishing contact between the air in the alveoli and the blood in the alveolar capillaries, which can be entered into physiological equations for predicting oxygen uptake. This information is provided by morphometric studies involving stereological methods and allows estimates of the pulmonary diffusing capacity of the human lung that agree, in experimental studies, with the maximal oxygen consumption. The basis for this "machine lung" structure lies in the complex design of the cells building an extensive air-blood barrier with minimal cell mass.

Keywords Lung morphometry · Gas exchange · Alveolar cells · Alveolar epithelium · Capillary endothelium

Introduction: searching for the structural basis of lung physiology

In 1956, the Nobel Prize for Physiology and Medicine was awarded to André F. Cournand and Dickinson W. Richards, together with Werner Forssmann, for their pioneering work with cardiac catheterization, which had an enormous impact on cardio-pulmonary physiology. Indeed, pulmonary physiology was different after the work of Cournand and Richards if only with regard to the new possibilities of sampling and studing mixed venous blood by inserting a catheter into the right auricle, thus allowing the chemical and physical study of the blood flowing into the pulmonary gas exchanger for oxygen uptake.

In his Nobel Lecture "Right heart catheterization" Richards said (Richards 1957): "*Measurements made in this exact location have provided a key to almost all the integrations that we have attempted in elucidating the nature of cardiopulmonary function.*" In his conclusions, he addressed the future of research in his field and, in particular: "*... (what) interests me greatly would be an effort to bring together function and structure, a reexamination of pulmonary anatomy by pathologists who are aware of functions and dysfunctions*".

When this was written, I was a young assistant in Zürich studying the anatomy and histology of bronchial-pulmonary arterial anastomoses, a hot topic in pulmonary pathology at the time (Loring and Liebow 1954; Fritts et al. 1961), raising questions as to their functional importance (Weibel 1958, 1959). In 1958, I was able to follow up this project as a postdoctoral fellow in the group of the lung pathologist Averill Liebow at Yale, during which time I was invited by Cournand to give a seminar on my studies at Bellevue Hospital in New York. After the seminar, Cournand and Richards formally invited me to come and work with them in their Cardio-Pulmonary Laboratory. When I asked what they expected me to do, Cournand said simply: "*Do anything on the structure of the lung that is of interest for physiology*", evidently Richards' vision but quite a challenge for a young Swiss anatomist. When they offered full support for the establishment of suitable laboratory facilities and to more than double my modest fellowship, I accepted.

However, what have anatomists missed that their research was not of sufficient interest to physiologists? This question arose when I joined the Cardio-Pulmonary Laboratory at Bellevue Hospital in September 1959. The answer soon became apparent when I met Domingo M. Gomez, a Cuban

✉ Ewald R. Weibel
weibel@ana.unibe.ch

[1] Institute of Anatomy, University of Bern, Baltzerstrasse 2, CH-3000 Bern 9, Switzerland

 Springer

cardiologist and Biomathematician who had fled the terror reign of Fidel Castro and been given refuge by Cournand. Over coffee, Gomez asked me questions, such as "how many alveoli are there in the human lung?" I had no real answers, as the numbers in the literature ranged from 60 to several hundred millions and the estimation methods used appeared to be ill founded, one problem being that alveoli are "seen" in the microscope only as two-dimensional profiles. Therefore, we first developed a geometrically sound method for counting such structures on two-dimensional sections (Weibel and Gomez 1962b) obtaining some 300 million alveoli in adult human lungs. This method held sway until 1984 when Sterio (1984) introduced the disector method for counting three-dimensional (3D) structures on sections and the number estimate remained valid until Ochs et al. (2004) applied a variant of this procedure to human lungs, increasing the now best estimate to 400 million.

Gomez turned out not to be really interested in knowing the number of alveoli; he wanted to know this value only for calculating the alveolar gas exchange surface area with a geometric model. However, by now, it had become clear what I was expected to add to the study of lung structure to make it "of interest for physiology", namely the quantification of all the relevant structures that determine the gas exchange conditions in the lung, from alveoli and capillaries to airways and blood vessels, a quantitative aspect of lung architecture and structure that we would then call "morphometry" (Weibel and Gomez 1962a; Weibel 1963).

Setting up quantitative structure-function relationships

Gomez saw the importance of this approach in view of his two major projects: the distribution of air flow in the airway tree (Gomez 1963) and the importance of structural design in setting up an efficient gas exchanger. I contributed to both (Weibel 1963) but will discuss only the second project.

Modeling gas exchange in the human lung was a hot topic at the time. The origin of the prevailing concept went back to Christian Bohr (1909) who formulated, in 1909, the basic gas exchange equation:

$$V_{O2} = (PA_{O2} - Pc_{O2}) \cdot DL_{O2} \qquad (1)$$

where the difference between P_{O2} in alveolar gas and capillaries was the driving force for gas flow with a conductance DL_{O2}, called the diffusing capacity, as the modulator. Bohr formulated this equation to find out whether O_2 is taken up by diffusion or by secretion, as was a prevailing opinion at the time (Haldane and Smith 1897) but his two young collaborators Marie and August Krogh soon established unambiguously that O_2 uptake occurs by diffusion (Krogh and Krogh

1910). This concept clearly indicated that, based on Ohm's law, DL_{O2} must be proportional to the gas exchange surface and inversely proportional to the tissue barrier thickness.

It took 50 years until Roughton and Forster (Roughton and Forster 1957) showed, in 1957, that this model was too simple and that the gas exchanger is made of two components that affect the physics differently: in addition to the passive diffusion barrier of the alveolar capillary membrane, the blood plays a central role in the binding of O_2, so that DL_{O2} is determined by two serial resistances: the diffusion barrier and the reactive erythrocytes in capillary blood. This now had introduced, in a formal way, structural parameters in this gas exchange equation and in 1959, Gomez wanted to take this one step further by introducing all structural components, accurately estimated, so that one could predict a theoretical value of the diffusing capacity from first principles. This was to be my challenge.

Exploring various model concepts (Weibel 1970; Weibel et al. 1993), we formulated a structure-function model on the basis of the equations of Bohr and of Roughton-Forster:

$$DL_{O2}^{-1} = DM_{O2}^{-1} + De_{O2}^{-1} \qquad (2)$$

where the serial conductances DM_{O2} and De_{O2} of the barrier and the blood, respectively, are of a highly different nature (Fig. 1). DM_{O_2} is the conductance of a diffusion barrier that offers "passive" resistance to diffusion driven by partial pressure gradients and thus depends essentially on the material properties of the barrier, as estimated by a diffusion coefficient K and on the dimensions of the barrier: the larger the surface area S and the thinner the barrier thickness τ, the greater DM_{O_2}. In contrast, De_{O_2} depends on the erythrocyte volume in capillaries but is related to a complex physico-chemical process that involves, in addition to diffusion, the binding rate of O_2 to hemoglobin (Roughton and Forster 1957; Holland et al. 1985; Yamaguchi et al. 1985).

Membrane conductance (DM_{O_2}) The structural characteristics of the membrane conductor are seen in Fig. 1. It is made up of the two layers that separate the air in alveoli from the erythrocytes in the capillary: namely the tissue barrier and the layer of blood plasma (Fig. 1a). In addition, an alveolar lining layer of variable thickness spreads over the epithelial surface (Fig. 1b) and modulates surface texture (Bachofen and Schurch 2001).

In the original model, the diffusion barrier was considered to be composed of two (or three) resistances in series: tissue (with the surface lining layer) and blood plasma (Weibel 1970). Even though the two layers of the barrier, namely tissue and plasma, are different, this does not appear to be important under normal conditions. For one thing, the flow velocity of the plasma layer is much lower than the diffusion of O_2, so that plasma is quasi-static with respect to diffusion (Federspiel
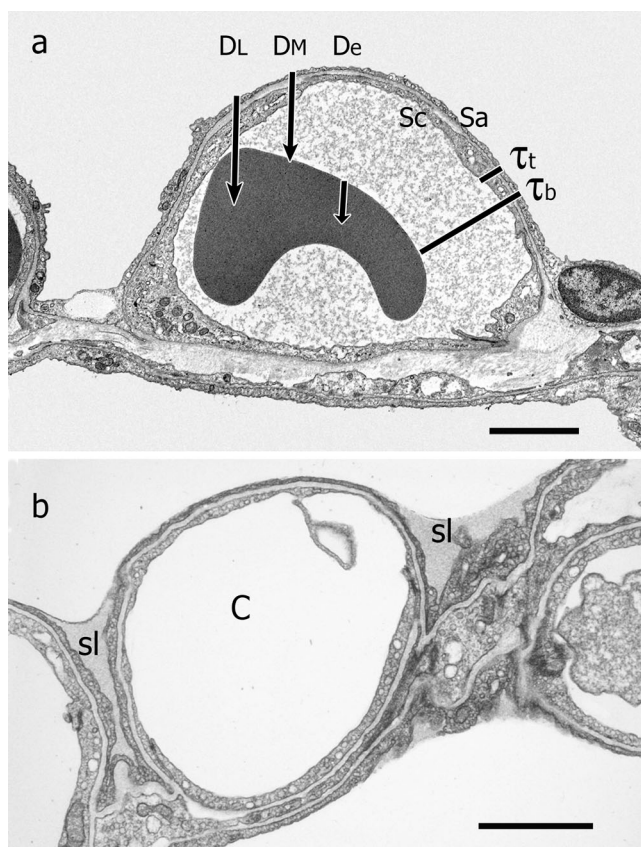
Fig. 1 **a** Electron micrograph of the alveolar capillary of instillation-fixed human lung showing the structural definition of the parameters of diffusing capacity DL) and its two components (DM, De): note the alveolar and capillary surface area (Sa, Sc), total barrier thickness (τ_b) and tissue barrier thickness (τ_t). **b** Alveolar capillary (C) of perfusion-fixed rabbit lung showing alveolar surface lining layer (sl) topped by fine surfactant film. *Bars* 2 μm

1989). Furthermore, under normal conditions, the surface areas of alveoli, capillaries, and erythrocytes differ little and the diffusion coefficients of tissue and plasma are also quite similar and so we can more reasonably treat them as a single barrier (Weibel et al. 1993). Accordingly, the membrane diffusing capacity is the diffusion conductance from the alveolar surface to the erythrocyte membrane (Fig. 1):

$$DM_{O_2} = K_b \cdot S(b) \, / \, t_{hb} = K_b \cdot (S(A) + S(c))/2 \cdot \tau_{hb} \quad (3)$$

where K_b is Krogh's permeation coefficient estimated at $3.3 \cdot 10^{-8} cm^2 \cdot min^{-1} \cdot mmHg^{-1}$. S(b) is the surface area of the barrier that we estimate as the mean of the alveolar and capillary surface areas, whereas S(A) and S(c), respectively, are the two most robust measures of the area of air-blood contact. The effective mean barrier thickness is the harmonic mean τ_{hb}, the mean of the reciprocals of the distance from the alveolar surface to the nearest erythrocyte membrane. The harmonic mean is chosen as a parameter for the diffusion resistance because the local rate of O_2 diffusion is inversely proportional to the diffusion distance (Weibel and Knight 1964; Weibel et al. 1993).

Erythrocyte conductance (De_{O_2}) The erythrocyte conductance for O_2 is primarily determined by the capillary blood volume and involves several coupled events: (1) the diffusion of O_2 through the erythrocyte membrane, (2) the diffusion of molecular oxygen and oxyhemoglobin within the red blood cell and (3) the non-linear chemical reaction of O_2 with hemoglobin, a reaction that depends on the degree of O_2 saturation. To account for this complexity, Roughton and Forster (1957) introduced a coefficient θ_{O_2}, namely the rate of O_2 fixation on hemoglobin per unit of pressure and blood volume:

$$De_{O_2} = \theta O_2 Vc \quad (4)$$

where Vc is the total capillary blood volume.

The specific conductance θ_{O_2} is a physico-chemical parameter estimated in vitro on whole blood. It is not a constant but is affected by various blood properties such as hemoglobin concentration and initial O_2 saturation (Holland et al. 1977). For normal human lungs and a hemoglobin content of 15 g/100 ml of blood, the value $\theta_{O_2} = 1.8 \, mlO_2 \, ml^{-1} \, min^{-1} \, mmHg^{-1}$ and is a reasonable estimate (Yamaguchi et al. 1985).

Lung structure serving gas exchange

This model analysis has now revealed the information from lung structure considered of interest for physiology and that we had previously failed to provide: the total surface area of contact between air and capillary blood, the effective thickness of the diffusion barrier and the volume of capillary blood and of erythrocytes. To obtain this information required a new approach to the structural study of the lung for two reasons (Weibel et al. 2007): (1) to study lung fine structure requires microscopy because the active regions, alveoli and capillaries, are very small but we had to account for the large size of the organ and this called for rigorous sampling procedures to ensure that the microscopic measurements accurately represented the make-up of the lung (Cruz-Orive and Weibel 1981; Weibel 1963; Weibel et al. 2007; Hsia et al. 2010); (2) tissue samples for microscopy are thin sections and the image we can study is a two-dimensional "profile" whereas the structures of interest are three-dimensional, so a method has to be found that relates the 2D images to 3D structures. In 1959, the solution to these problems was not immediately evident.

To satisfy the first requirement, the lung must be fixed and prepared under standardized "near-physiological" conditions. In 1959, we fixed the lungs by formalin steam (Weibel and Vidone 1961) to obtain specimens representing the physiological conditions of controlled inflation and perfusion. This was good for light microscopy but did not provide specimens suitably fixed for high-resolution electron microscopy, as required for the model analysis. Here, the solution was instillation

fixation with glutaraldehyde under controlled pressure (Fig. 1a); this retains the blood in capillaries (Vock and Weibel 1993) and allows the measurement of the required parameters. Unfortunately, it abolishes the surface lining layer of alveoli with surfactant that can only be demonstrated by vascular perfusion of the fixative (Weibel and Gil 1968; Bachofen et al. 1982), which fixes the fine layer "from behind" but removes the blood (Fig. 1b).

The second problem was finding a method with which to obtain 3D parameters from measurements that we could only carry out on 2D sections. Gomez wanted to calculate the surface area from the number of alveoli with a geometric model. However, we found that such approximate calculations were not necessary, because of the availability of a method for estimating the 3D surface area of alveoli by measurements on sections (Campbell and Tomkeieff 1952; Elze and Hennig 1956) by simply counting intersections of the surface with random test lines placed on the section (Fig. 2). Moreover, 3D volumes can be estimated from sections by point counting on random test point grids, a method long used in mineralogy to determine the composition of rocks. These are the basic methods of "stereology", a set of mathematically based microscopic measuring methods that were developed just around the time that we were engaging in these studies; the term stereology was coined in 1961 (Weibel and Elias 1967) and this would bring us a wealth of new methods by which to add numbers to the study of fine structure extending way beyond the lung (Weibel 2013a, b; Ochs 2006; Weibel 1979; Baddeley and Jensen 2005; Pakkenberg and Gundersen 1995; Hsia et al. 2010).

Morphometry of human lung in relation to diffusing capacity

With this model and these methods proceeding in hand, we could, in principle, attempt to estimate a theoretical value of the diffusing capacity of the human lung on the basis of morphometric data but this was not as easy as it looked; it took many years to assemble a set of normal human lungs, suitably prepared *post mortem* to allow a study by electron microscopic morphometry (Gehr et al. 1978; Weibel et al. 1993). The data obtained from young adults of average body mass 70 kg (Table 1) revealed the alveolar surface area to amount to 130 m^2 and the capillary surface to be about 10 % smaller; these values were higher than the older data from 1963 (Weibel 1963) as these had been derived from light microscopic studies that did not adequately resolve the alveolar surface texture. The mean thickness of the tissue barrier is 2.3 μm but the effective thickness for diffusion is the harmonic mean thickness, which is 0.6 μm, whereas the harmonic mean total barrier thickness, measured from alveolar to red cell surface (Fig. 1a), amounts to 1.11 μm. The capillary volume is estimated at about 200 mL. With these data, we calculate D_{LO_2} for the adult human lung to be about 150 mL O$_2 \cdot$ min$^{-1} \cdot$ mmHg^{-1} (Weibel 2009; Hsia et al. 2016).

These morphometric estimates of the diffusing capacity are based on model assumptions. The test of their validity must be to compare them with physiological estimates. The standard physiological value of DL_{O_2} of a healthy adult at rest is about 30 ml O$_2$/min-1/mmHg-1 but this is not a valid comparison. The pulmonary capacity for diffusive O$_2$ uptake must be gauged to satisfy the largest achievable metabolic rate, because the structural features determining DL_{O2} cannot be increased at short notice when demand imposed by the working cells, for example, muscle, increases in physical activity. A number of estimates have been made for DL_{O2} in exercising humans and these have yielded values of the order of 100 ml O$_2 \cdot$ min$^{-1} \cdot$ mmHg^{-1} (Hammond and Hempleman 1987). The fact that this is only about 50 % lower than the morphometric estimate is not disturbing, for we do not know whether the "true diffusing capacity" is completely exploited, even in heavy exercise. More informative may be comparative physiology studies in which DL can be estimated both by
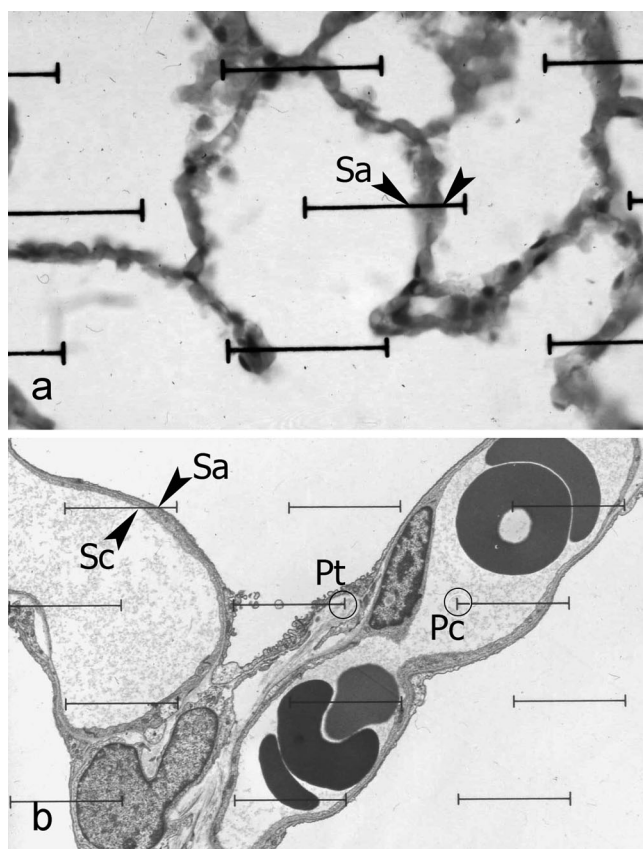

Fig. 2 **a** Light micrograph of human lung with test line system for estimating alveolar surface area from intersection points, as used in 1959. **b** Same test system applied to electron micrograph of human lung allowing the estimation of alveolar and capillary surface areas, *Sa* and *Sc* and of capillary and tissue volumes by point counting, *Pc* and *Pt*. *Testlines* used as *bars* 120 μm (**a**), 6 μm (**b**)

Table 1 Morphometric estimate of DL_{O_2} for healthy adults of 70 kg body weight and measuring 175 cm in height[a]

Measured parameter	Mean	± 1 SE	Unit
Morphometric data (mean ± 1 SE)			
Total lung volume (60% TLC)	4340	± 285	ml
Alveolar surface area	130	± 12	m^2
Capillary surface area	115	± 12	m^2
Capillary volume	194	± 30	ml
Air-blood tissue barrier thickness			
Arithmetic mean	2.20	± 0.2	μm
Harmonic mean	0.62	± 0.04	μm
Total barrier thickness			
Harmonic mean	1.11	± 0.1	μm
Conductances			
Membrane, D_{MO_2}	332	-	ml/min per mmHg
Erythrocytes[b], D_{EO_2}	319	-	ml/min per mmHg
Total, DL_{O_2}	163	-	ml/min per mmHg

[a] From Gehr et al. (1978) and Weibel et al. (1993)

[b] With $\theta_{O_2} = 1.5$ ml/ml per min per mmHg (Holland et al. 1977)

morphometry and by physiological methods by using tracer gases. One such set of studies is the assessment of the functional loss of gas exchange capacity following the reduction of the gas exchange structure by partial pneumonectomy in dogs (Hsia 2006; Hsia et al. 1993). These studies have shown that the functional estimate of DL_{CO} under heavy exercise conditions agrees with the morphometric estimate (Fig. 3). This general finding has been confirmed in further studies (Hsia 2006) and so, we can accept the theoretical estimate of DL_{O2} in general and for the human lung in particular as

Fig. 3 Physiological estimates of DL_{CO} by rebreathing in exercising dogs reach the morphometric estimate when blood flow reaches its maximum at top running speed. Data from Carlin et al. (1991) and Hsia et al. (1993)

reflecting the limit to O_2 uptake imposed by the structural parameters of the gas exchanger.

Biology behind a physi(ologi)cal gas exchanger

This attempt to make morphology useful for physiology revealed that a simple combination of morphometric parameters allows the prediction of the functional capacity of the lung: the essential features of the lung for gas exchange are an astonishingly large internal surface of nearly the size of a tennis court in humans combined with an excessively thin tissue barrier that must support the capillaries in air space, with 0.2 μm related to 130 m^2 having a ratio of 8 orders of magnitude in linear dimensions.

This is certainly impressive but for a biologist, the reduction of the "physiologically relevant" aspects of the lung to a few numbers is not satisfactory. The questions are how has this come about, how can this large surface become built into the restricted space of the chest and, in particular, what cells contribute to build and maintain the structure supporting this large surface with so little tissue over a lifetime. The key to these puzzles is lung development, which leads to a well-structured hierarchical order in the elements building the lung. The process is governed by the progressive dichotomous branching of the airway tubes over 23 generations, on the average, to build a space-filling system of airways from the trachea to the terminal air sacs showing the characteristics of a fractal tree (Weibel and Gomez 1962a, b; Weibel 2013a, b; Weibel 1991). The first 15 generations provide conducting airways, bronchi and bronchioles, whereas the last eight
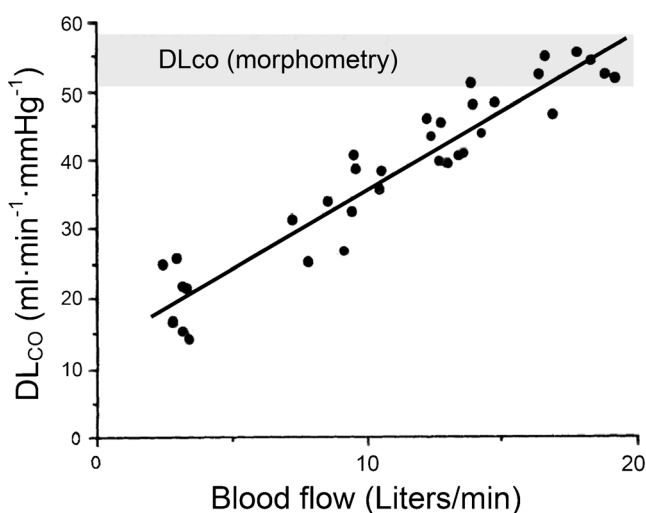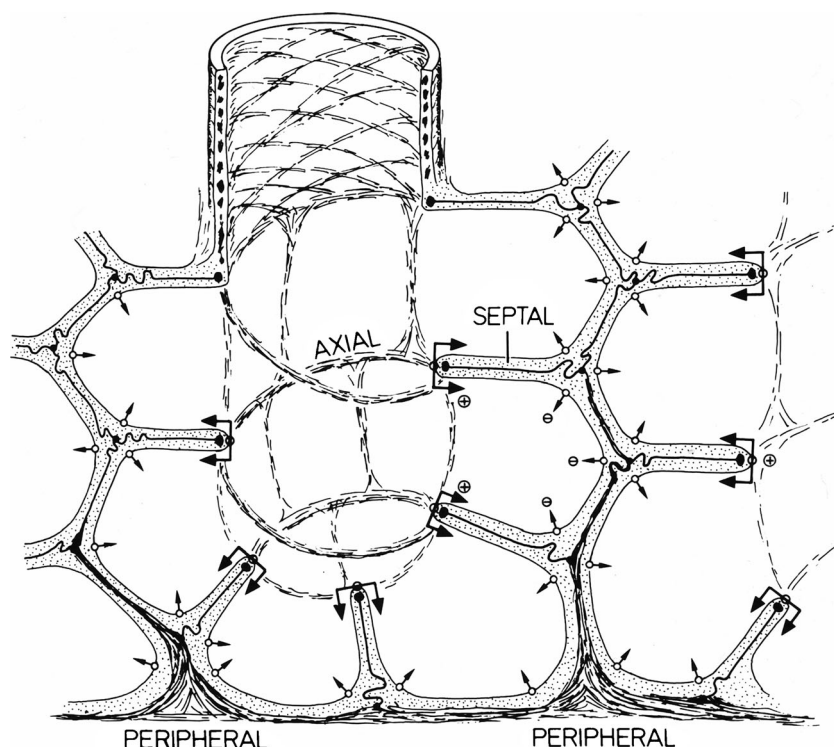
Fig. 4 Model of the disposition of axial, septal and peripheral fibers in the acinar airway, with the effect of surface forces being indicated by *arrows*: these forces are negative in the alveoli and strongly positive on the free edge of the alveolar septum. Reprinted by permission from Weibel (1984)

generations become transformed into the gas exchanging modules, the acini, when the smooth walls of air ducts form septa thus building a sleeve of alveoli whose walls contain single capillaries, a process called alveolarization, which increases the alveolar surface area drastically in a short time (Burri et al. 1974; Burri 2006).

In concert with the airways, the pulmonary arteries and veins branch and finally form the capillary network within the alveolar septa. As this happens, the loose mesenchyme gradually forms a fine coherent scaffold that extends from the hilum all the way to the visceral pleura. It traverses the alveolar septa as a fine fiber meshwork that supports the capillary network (Fig. 4). These septal fibers are anchored on two more robust fiber systems: (1) the axial fibers that are part of the wall of airways and follow into the acinus as the fiber network forming the alveolar entrance rings on the alveolar ducts and (2) the peripheral fibers that penetrate into the acini from the pleura and the interlobular septa (Fig. 4). An important consequence of this hierarchical structure is that the septal fiber strands that support the

Fig. 5 Model of an alveolar capillary network (*red*) with interweaving connective tissue fibers (*green*). *Bar* 5 μm

capillaries (Fig. 5) can be rather short and therefore also very thin, an important feature for keeping the barrier thin in view of gas exchange.

What cells do to make a good lung—other insights from morphometry

Even though the alveolar tissue is extraordinarily slim, it is built by cells serving various functions, as shown in Fig. 6. Two cells form the air-blood barrier, namely the endothelial cell that lines the capillaries and the type 1 alveolar epithelial cell that forms the lining of the alveolar space (Fig. 6b). The alveolar epithelium also comprises the cuboidal type 2 cell that is the secretory cell responsible for the formation of the surfactant lining (Fig. 6a). The interstitial space between the epithelial and endothelial cells, bounded by their basement membranes, contains the fibroblasts responsible for the formation and maintenance of the fiber system (Fig. 6a). The alveolar macrophage (Fig. 6c) is loosely attached to the epithelial surface and forms lamellipodia on its advancing edge with which it moves over the surface and phagocytoses foreign materials. It is by far the largest alveolar cell and is a constituent of the alveolar surface lining layer (Fig. 6c, inset).
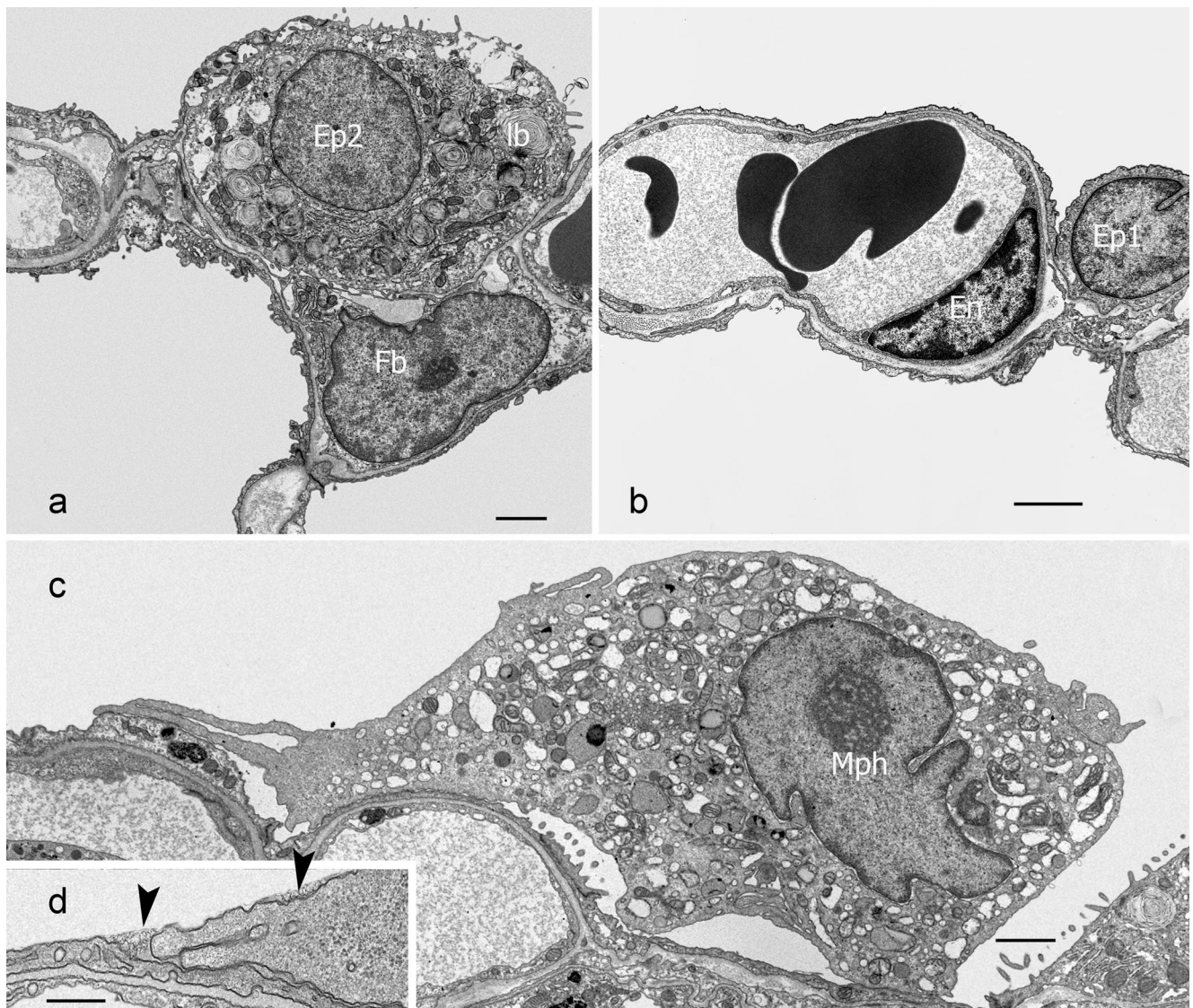

Fig. 6 Cells of the alveolar region as seen in electron micrographs. **a** Type 2 epithelial cell (*Ep2*) with lamellar bodies (*lb*) together with a fibroblast (*Fb*) in human lung. **b** Capillary with endothelial cell (*En*) and type 1 epithelial cell (*Ep1*) that constitute the diffusion barriers in a dog lung. **c** Alveolar macrophage (*Mph*) in human lung is the largest cell loosely attached to the epithelium and shows two lamellipodia on the advancing edge to the *left*. **d** Advancing lamellipodia of a macrophage in a perfusion-fixed rabbit lung are covered by the surface lining film (*arrowheads*). *Bars* 2 μm (**a–c**), 0.2 μm (**d**)
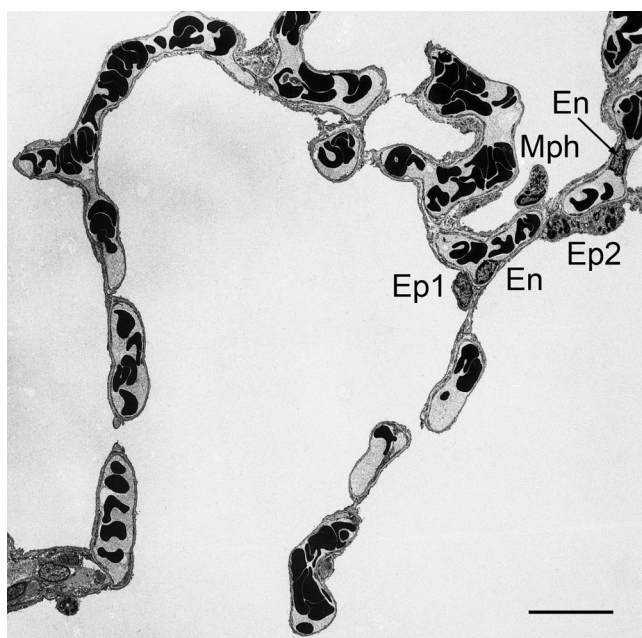
Fig. 7 Low-power view of an alveolus of a dog lung showing very few cell bodies: two endothelial cells (*En*) and one each of the epithelial cells type 1 (*Ep1*) and type 2 (*Ep2*) and one macrophage *(Mph)*. *Bar* 20 μm

Fig. 8 Diagram showing the ramified cytoplasmic extensions (*red*) of an endothelial cell with one nucleus (*blue*) lining the capillary network. *Bar* 5 μm

All these cells are, however, very rare as seen in an electron micrograph of an alveolus of a dog lung (Fig. 7): in this image, we find no more than two endothelial cells and one each of the type 1 and 2 epithelial cells, plus one macrophage but no fibroblasts; the largest part of the alveolar wall surface is built only of the thin cytoplasmic extensions of endothelial and type 1 epithelial cells with a very thin interstitium separating them. This is the reason that some prominent lung histologists long believed that the alveolar surface was "naked like a wound" (Eberth 1862; Policard 1929): the thin barrier parts measure no more than 0.2 to 0.4 μm, which was just at the resolution limit of the light microscope. It was the pioneer of lung electron microscopy Frank Low (1911–1998) who showed, in 1953, that the alveoli in mice and humans were lined by an uninterrupted epithelium made of two cell types: a "large" cuboidal cell with the features of a secretory cell and a "small" squamous cell that lined the capillaries with very thin cytoplasmic leaflets (Low 1953). We will see that the "large" type 2 cell is indeed much smaller than the type 1 cell. This
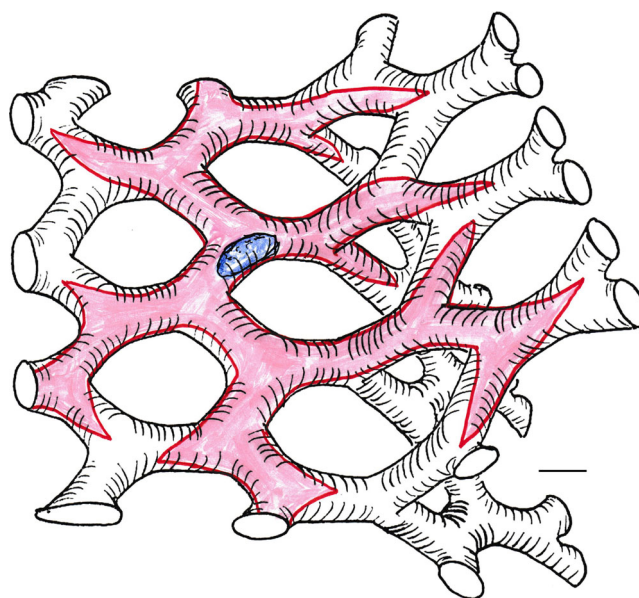
discovery with the new tool electron microscope was soon confirmed by one of the original proponents of the "naked" view in a paper published in this journal (Policard et al. 1959).

This pictorial observation was corroborated by a morphometric study of the cell population of the human alveolar region (Crapo et al. 1982). As shown in Table 2, each of the 400 million alveoli is served by no more than 47 type 1 alveolar epithelial cells and 92 type 2 cells and is, thus, a mosaic with a total of 140 epithelial cells, whereby the type 1 cells cover 95 % of the surface of 220,000 μm² of an average alveolus. Similarly, the capillaries in the alveolar walls are lined by 170 endothelial cells and one finds 210 interstitial fibroblasts and no more than 57 macrophages associated with these structures. This means that each type 1 cell must cover a surface of 5098 μm² of the alveolar septum, a very large surface indeed compared with less than 100 μm² for a typical cuboidal epithelial cell. Accordingly, the total cell volume of a type 1 cell is twice as large as that of the "large" type 2 cell, although it covers a surface 30 times larger (Table 2).

Table 2 Number and size of alveolar cells in human lung. After Crapo et al. (1982)

Cells/structure	n (total) ×10⁹	Mean volume μm³	n/alveolus	Mean S(basal)[a] μm²	Mean thickness μm
Alveolar epithelial cell type 1	19	1763	47	5098	0.36
Alveolar epithelial cell type 2	37	889	92	183	5.03
Endothelium	68	632	170	1353	0.48
Interstitial cells	84	637	210	–	–
Macrophages	23	2491	57	–	–

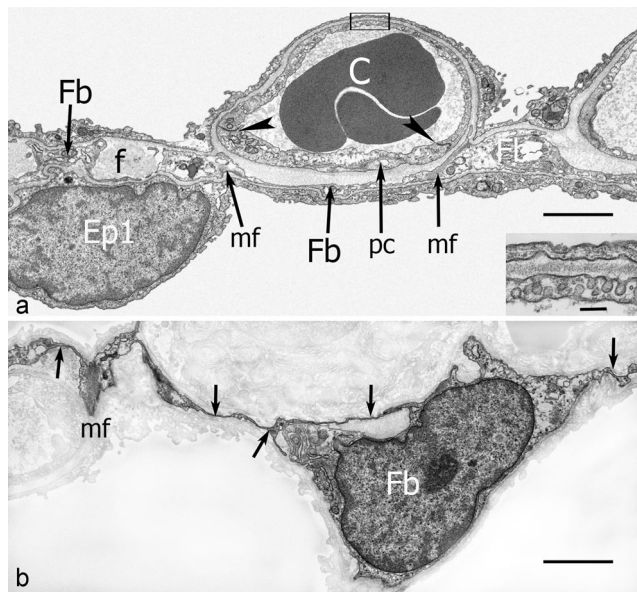[a] Surface of basal cell membrane attached to basement membrane

Fig. 9 a Alveolar septum of human lung showing a capillary (*C*) with two intercellular junctions of the endothelium (*arrowheads*) and a pericyte process (*pc*), a type 1 epithelial cell (*Ep1*) and fine extensions of a fibroblast (*Fb*) that is tightly related to fibers (*f*) and forms myofibrils (*mf*) that span across the septum. The *box* marks the minimal barrier whose structure is shown in the *inset*: the epithelium and endothelium are joined by their fused basement membranes. **b** Touched-up image of the fibroblast in Fig. 6a to show the very slim cytoplasmic extensions (*arrows*). Bars 2 μm (**a**, **b**), 0.1 μm (*inset*)

Capillaries and interstitial cells

The alveolar capillaries are lined by a continuous endothelium in the form of thin leaflets that emanate from the central cell body with a nucleus (Fig. 6b), each cell having an expanse of 1350 μm² on the capillary surface. Considering the geometry

of the alveolar capillary network (Fig. 8) with segments no more than 6 μm in diameter and 8 μm long (Weibel 1963), we must assume that the endothelial cell spreads its cytoplasmic leaflets along the meshes of the capillary network in the form of branched thin strips because, on cross-sections of capillaries, one usually finds two to three intercellular junctions (Fig. 9a). This means that, generally, two endothelial cells participate in lining a capillary tube. The capillary endothelium is attached to a thin basement membrane; the rare pericytes (Fig. 9a) are associated with the endothelial basement membrane and are located on the surface facing the interstitial space.

The basement membranes of the endothelium and the alveolar epithelium form the boundary of the interstitial space that contains the fiber system and the fibroblasts. Of particular interest is that the interstitial space is obliterated over about half of the capillary surface where the epithelial and endothelial basement membranes are fused (Fig. 9a, inset) thus forming the minimal gas exchange barrier (Figs. 1, 6a, 9a); thicker barrier regions that contain the fibers and the fibroblasts are limited to the other half of the capillary surfaces but this alternates sides as the fibers are interwoven with the capillary network (Fig. 5).

The alveolar fibroblasts are particularly complex cells. Their volume is about the same as that of endothelial cells (Table 2) but it turns out that they are very heavily ramified with extremely thin cytoplasmic strips (Fig. 9b) that enwrap the fiber strands and form actomyosin bundles of the smooth muscle type (Fig. 9a); these contractile elements give the fibroblast the quality of a "myofibroblast" (Kapanci et al. 1974) but, notably, their orientation is crosswise connecting the two epithelial linings between capillary meshes (Fig. 9a); their putative function is to serve as braces of the interstitial space.

Fig. 10 Scanning electron micrograph of the alveolar surface of a human lung showing protruding capillaries and two type 2 cells (*Ep2*) sitting in niches and characterized by a rim of microvilli. The *small arrow* indicates the cell body of a type 1 cell (*Ep1*) that covers several capillary meshes (*yellow*); the boundary of its cytoplasmic leaflet is marked by *arrowheads* outlining a small lip of the cell junction between adjoining cells (*inset*). The surface area covered by this cytoplasmic leaflet is 1300 mm². Reproduced by permission from Weibel (2015). *Bar* 10 μm
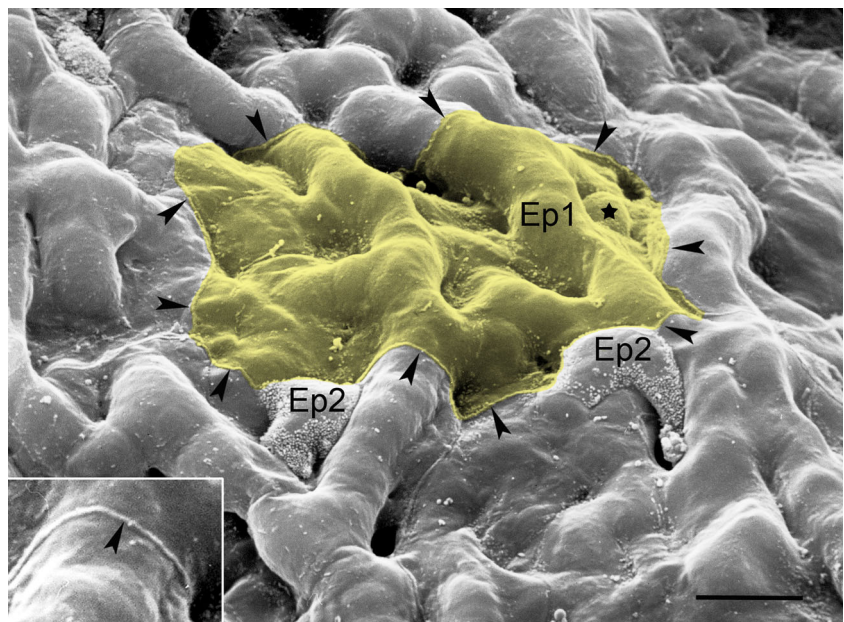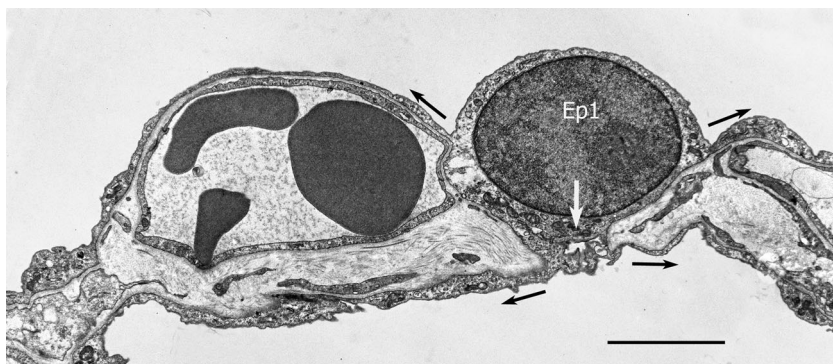
Fig. 11 Alveolar septum from monkey lung showing a type 1 epithelial cell (*Ep1*) that forms the lining of both sides of the septum by extending with a cytoplasmic stalk to the lower side (*arrows*). *Bar* 5 μm

Alveolar epithelial cells—champion optimizers

The type 1 alveolar epithelial cell is twice as large in volume as the "large" type 2 cell (Table 2); the major part of this volume is found in the thin cytoplasmic leaflets (Fig. 6b) that spread over the basement membrane over an area of 5100 μm², which is nearly four times larger than an endothelial cell, even though the two lining cells cover the same area and are extremely tightly associated by their fused basement membranes over about half the surface (Fig. 9a). Scanning electron micrographs of the alveolar surface (Fig. 10) show the mosaic of the two epithelial cell types and reveal the outline of the cell boundaries by the terminal bars (Fig. 10). Similar to the endothelial cell (Fig. 8), the type 1 epithelial cell shown here covers several meshes of the capillary network with its thin lamella but the cell area seen here is only 1300 μm² and thus is only ¼ of the average cell surface area found by morphometry. This is perplexing but is in agreement with the observation by Albert Kölliker in 1881 that there were many more cytoplasmic patches of the alveolar epithelium than there were nuclei, an observation made by silver staining the terminal bars (Kölliker 1881). Kölliker concluded that the major part of the alveolar epithelium was made of "non-nucleated cytoplasmic plates", an alternative view to the "naked" alveolar surface discussed above.

It turns out that this was a correct observation but an erroneous conclusion (Weibel 1971, 2015). Type 1 cells are not simple squamous cells as may appear in "typical" micrographs such as Figs. 1, 6b, 9. As shown in Fig. 11, they can be branched forming a broad cytoplasmic sheet on the top surface of the alveolar wall but then extending across the capillary mesh to the other side with a cytoplasmic stalk to form another cytoplasmic sheet on the surface of the adjoining alveolus, whereby each of these sheets is bounded by a terminal bar or tight junction to the adjoining cell. Hence, this makes two "cytoplasmic plates" of Kölliker but both are connected to the nucleus and are therefore not "non-nucleated". Moreover, each type 1 cell can make several such branches that cross over to the other side (Fig. 12). By means of this arrangement, the type 1 cells can form leaflets only about 0.1 μm thick extending over 5000 μm² with a single nucleus as the metabolic center (Weibel 2015). However, this has serious consequences: the architecture of the type 1 cell is now characterized by having multiple apical membrane areas; accordingly, the cell has lost the typical polarity of epithelial cells that extends between the well-matched apical and basal membrane, a feature most important for orderly cell division during mitosis. As a consequence, type 1 cells are unable to divide and multiply mitotically, neither during repair when they must be regenerated from stem cells, nor during
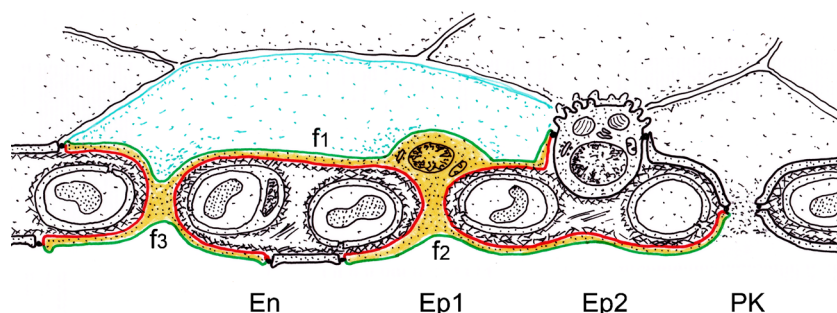

Fig. 12 Diagram of a section of an alveolar septum with the branched type 1 cell (*yellow*) forming the cytoplasmic plates: *f1* (comprising the nucleus) and *f2* plus *f3* (connected with stalks to the nuclear area). The apical cell membrane is shown in *green* and the basal membrane in *red*, separated by the terminal bar (*black dots* terminal bar, *En* endothelial cell, *Ep1* type 1 epithelial cell, *Ep2* type 2 epithelial cell, *PK* pore of Kohn). Reproduced by permission from Weibel (2015)

Fig. 13 Alveolar septum of human lung showing a type 1 epithelial cell (*Ep1*) extending across a pore of Kohn to a junction on the lower surface (*arrowhead*). The type 2 cell (*Ep2*) is also related to both alveoli. Note residual surfactant material in the alveolar pore. *Bar* 5 μm
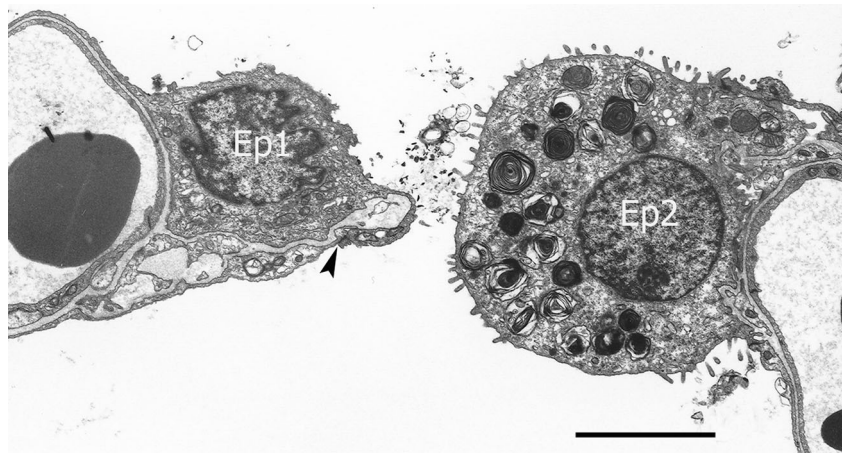
development when the increasing alveolar surface needs more cells: after mitotic division, some of the new type 2 cells transform into the squamous type 1 cells (Kapanci et al. 1969; Kauffman et al. 1974; Evans et al. 1975).

The opportunity for establishing this complexity lies in the design of the alveolar wall with its minimized interstitial scaffold. This wall is characteristically perforated by pores of Kohn that connect neighboring alveolar spaces and are usually filled with alveolar lining fluid. This is the place at which the alveolar epithelium can "move" from one side to the other. Figure 13 shows such a pore from a human lung; a type 1 cell extends its leaflet to the other alveolus and a type 2 cell sits between the two alveoli. Remnants of alveolar lining fluid can be seen in the pore.

This differentiation of alveolar epithelial cells is highly conserved in mammalian species. The basal surface of type 1 cells is rather invariant, independent of body size, with 5320, 4004 and 5340 μm^2 in humans, baboons, and rats, respectively (Crapo et al. 1982) and with an average of 6000 μm^2 across 10 species from the shrew at 3 g to the horse at 500 kg (Stone et al. 1992). In the Etruscan shrew with its tiny alveoli and high alveolar surface area (Gehr et al. 1980), the complexity of type 1 cells is particularly high, suggesting that, in this animal with its particularly high metabolic rate, the optimization of gas exchanger structure has been pushed to extremes (Weibel 2015).

Separating barrier and secretory functions

Both the alveolar epithelium and the endothelium must serve as a minimal diffusion barrier and perform some secretory functions. Whereas the design for the barrier function minimizes the depth of the cell lining in both cases, minimizing even the perinuclear cytoplasm that contains a few organelles (Figs. 1, 6b, 9, 11), the secretory functions demand the activity of the cytoplasmic organelle system for the synthesis, packaging and

storage of the secretory products; this must significantly increase the bulk of the secretory cells. In the alveolar epithelium,
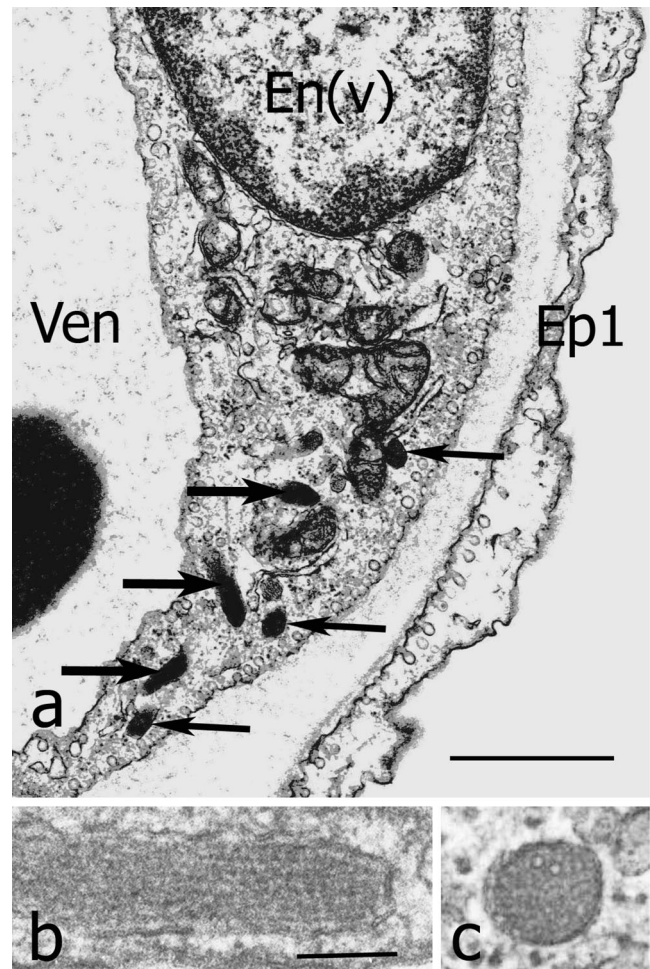

Fig. 14 a Endothelial cell (*En(v)*) of a small pulmonary venule (*Ven*) containing several rod-shaped Weibel-Palade bodies (*arrows*) that store von Willebrand protein. **b**, **c** Longitudinal and transverse sections, respectively, of the Weibel-Palade bodies at higher resolution to show the tubular structure formed by spiraled von Willebrand protein strands. *Bars* 1 μm (**a**), 0.1 μm (**b**, **c**)

the secretory function is assigned exclusively to the type 2 cells with their rich endowment of endoplasmic reticulum and Golgi complex generating the lamellar bodies as storage organelles for surfactant (Figs. 6a, 13; Mason and Shannon 1997; Ochs et al. 2002; Ochs 2010). These bulky cells occupy no more than 5 % of the alveolar surface area and are mostly tucked away in niches or capillary meshes (Fig. 10); they thus inhibit diffusion by their bulk insignificantly. The secretory functions of vascular endothelia are related to the control of clotting, primarily by the von Willebrand protein, which is packed into rod-shaped secretory storage organelles, the Weibel-Palade bodies (Fig. 14; Weibel 2012); these organelles are assembled in the Golgi complex and secreted in an emergency when the vascular wall is damaged (Metcalf et al. 2008; Wagner and Frenette 2008). The secretory activity of endothelial cells and the occurrence of Weibel-Palade bodies are, however, limited to arterial and venous vessels, both in the pulmonary and in the systemic circulation; they are totally absent from capillary endothelial cells (Fuchs and Weibel 1966; Weibel 2012) and thus, the endothelial secretory function lies outside the diffusion areas in the lung and in other organs. Capillary endothelia represent a special phenotype of vascular endothelia and this remarkable fact should be taken into consideration when endothelial cells are used in synthetic lung models; substitution by non-capillary endothelial cells such as HUVEC (Ren et al. 2015) may not be adequate.

Concluding remarks

From the physiologist's perspective, the design of the pulmonary gas exchanger is a simple matter: a modest volume of circulating blood exposed to air over a sufficiently large surface and across an extremely thin tissue barrier. Morphometry can provide this information, and it is, indeed, one of the essential responsibilities of morphologists to ensure that such information is based on sound morphology, with respect both to the methods used (Hsia et al. 2010) and to the knowledge-based interpretation of structure (Ochs 2010).

However, for a biologist, this purely quantitative or engineering view is not satisfactory, because this "machine lung" must be built and maintained by cells, be repaired from within in case of damage and perhaps be adapted to different functional demands or conditions. This, in fact, is the real challenge of lung design (Hsia et al. 2016). Here again morphometry can make a significant contribution as evidenced by the discovery of the unusual topology and size of all cells that constitute the alveolar tissue, ensuring its integrity while allowing a thin but extensive diffusion barrier to form. This was discovered, in the first place, by estimating the number and sizes as well as the volumes and surfaces of these cells in the mature lung (Crapo et al. 1982; Stone et al. 1992) and,

then, by measuring the dimensional changes of lung cells while the alveolar surface area grows exponentially in early lung development (Burri et al. 1974; Kauffman et al. 1974).

When looking into the future, I like to paraphrase the plan of Dickinson Richards (Richards 1957) that led to the development of lung morphometry: "... *what interests me greatly would be an effort to bring together molecular cell biologists with a sense for structure and morphologists with a sense for function and dimensions to address and solve the question how lung cells develop a complex shape to establish a large surface with minimal cell mass.*" Such a plan must address the transformation of alveolar epithelial cells, newly formed by mitosis of type 2 cells during repair and development (Borok et al. 2011; Rock and Hogan 2011), from a secretory cell to a lining cell, switching off the secretory program in favor of one for broad cytoplasmic extensions with an expanse that is independent of body size, even when the diameter of alveoli varies between 50 and 500 μm between a shrew and a horse. This challenge must extend morphometry to the subcellular dimension and to higher complexities. Opportunities to achieve this goal are offered by the new 3D electron microscopy methods such as serial-block-face scanning electron micoscopy (SBF-SEM) or focused-ion-beam electron microscopy (Ochs et al. 2016), which produce large stacks of well-matched serial sections at high resolution. These allow the reconstruction of the 3D internal structures in great detail; however, the major challenge will be to extract quantitative information on these spatial complexities by using stereological methods adapted to such imaging modalities (Vanhecke et al. 2007).

Another major challenge for the further development of functional morphology will be to identify morphometric characteristics associated with the cellular biomarkers used for genetic and systems analyses, so as to link these features to the functional importance of cell and organ structure as a major contribution to what has been called morphomics (Lucocq et al. 2015; Mayhew and Lucocq 2015). This may be a concept of particular importance in an organ such as the lung in which the shape and dimensions of the cells are essential determinants of functional capacity.

References

Bachofen H, Schurch S (2001) Alveolar surface forces and lung architecture. Comp Biochem Physiol A Mol Integr Physiol 129:183–193

Bachofen H, Ammann A, Wangensteen D, Weibel ER (1982) Perfusion fixation of lungs for structure-function analysis: credits and limitations. J Appl Physiol Respir Environ Exerc Physiol 53:528–533

Baddeley A, Jensen EBV (2005) Stereology for statisticians. Chapman and Hall/CRC, Boca Raton

Bohr C (1909) Über die spezifische Tätigkeit der Lungen bei der respiratorischen Gasaufnahme und ihr Verhalten zu der durch die

Alveolarwand stattfindenden Gasdiffusion. Skand Arch Physiol 22: 221–280

Borok Z, Whitsett JA, Bitterman PB, Thannickal VJ, Kotton DN, Reynolds SD, Krasnow MA, Bianchi DW, Morrisey EE, Hogan BL, Kurie JM, Walker DC, Radisky DC, Nishimura SL, Violette SM, Noble PW, Shapiro SD, Blaisdell CJ, Chapman HA, Kiley J, Gail D, Hoshizaki D (2011) Cell plasticity in lung injury and repair: report from an NHLBI workshop, April 19-20, 2010. Proc Am Thorac Soc 8:215–222

Burri PH (2006) Structural aspects of postnatal lung development—alveolar formation and growth. Biol Neonate 89:313–322

Burri PH, Dbaly J, Weibel ER (1974) The postnatal growth of the rat lung. I. Morphometry. Anat Rec 178:711–730

Campbell H, Tomkeieff SI (1952) Calculation of the internal surface of a lung. Nature 170:116–117

Carlin JI, Hsia CC, Cassidy SS, Ramanathan M, Clifford PS, Johnson RL (1991) Recruitment of lung diffusing capacity with exercise before and after pneumonectomy in dogs. J Appl Physiol 70:135–142

Crapo JD, Barry BE, Gehr P, Bachofen M, Weibel ER (1982) Cell number and cell characteristics of the normal human lung. Am Rev Respir Dis 126:332–337

Cruz-Orive LM, Weibel ER (1981) Sampling designs for stereology. J Microsc 122:235–257

Eberth CJ (1862) Ueber den feineren Bau der Lunge. Z Wiss Zool 12:1–32

Elze C, Hennig A (1956) Inspiratory enlargement of volume and inner surface of the human lung. Z Anat Entwicklungsgesch 119:457–469

Evans MJ, Cabral LJ, Stephens RJ, Freeman G (1975) Transformation of alveolar type 2 cells to type 1 cells following exposure to NO2. Exp Mol Pathol 22:142–150

Federspiel WJ (1989) Pulmonary diffusing capacity: implications of two-phase blood flow in capillaries. Respir Physiol 77:119–134

Fritts HW Jr, Harris P, Chidsey CA 3rd, Clauss RH, Cournand A (1961) Estimation of flow through bronchial-pulmonary vascular anastomoses with use of T-1824 dye. Circulation 23:390–398

Fuchs A, Weibel ER (1966) Morphometric study of the distribution of a specific cytoplasmatic organoid in the rat's endothelial cells. Z Zellforsch Mikrosk Anat 73:1–9

Gehr P, Bachofen M, Weibel ER (1978) The normal human lung: ultrastructure and morphometric estimation of diffusion capacity. Respir Physiol 32:121–140

Gehr P, Sehovic S, Burri PH, Claassen H, Weibel ER (1980) The lung of shrews: morphometric estimation of diffusion capacity. Respir Physiol 40:33–47

Gomez DM (1963) A mathematical treatment of the distribution of tidal volume throughout the lung. Proc Natl Acad Sci U S A 49:312–319

Haldane JS, Smith JL (1897) The absorption of oxygen by the lungs. J Physiol (Lond) 22:231–258

Hammond MD, Hempleman SC (1987) Oxygen diffusing capacity estimates derived from measured VA/Q distributions in man. Respir Physiol 69:129–147

Holland RA, Hezewikj W van, Zubzanda J (1977) Velocity of oxygen uptake by partly saturated adult and fetal human red cells. Respir Physiol 29:303–314

Holland RA, Shibata H, Scheid P, Piiper J (1985) Kinetics of O2 uptake and release by red cells in stopped-flow apparatus: effects of unstirred layer. Respir Physiol 59:71–91

Hsia CCW (2006) Quantitative morphology of compensatory lung growth. Eur Respir Rev 15:148–156

Hsia CC, Fryder-Doffey F, Stalder-Nayarro V, Johnson RL Jr, Reynolds RC, Weibel ER (1993) Structural changes underlying compensatory increase of diffusing capacity after left pneumonectomy in adult dogs. J Clin Invest 92:758–764

Hsia CC, Hyde DM, Ochs M, Weibel ER (2010) An official research policy statement of the American Thoracic Society/European Respiratory Society: standards for quantitative assessment of lung structure. Am J Respir Crit Care Med 181:394–418

Hsia CC, Hyde DM, Weibel ER (2016) Lung structure and the intrinsic challenges of gas exchange. Compr Physiol 6:827–895

Kapanci Y, Weibel ER, Kaplan HP, Robinson FR (1969) Pathogenesis and reversibility of the pulmonary lesions of oxygen toxicity in monkeys. II. Ultrastructural and morphometric studies. Lab Invest 20:101–118

Kapanci Y, Assimacopoulos A, Irle C, Zwahlen A, Gabbiani G (1974) "Contractile interstitial cells" in pulmonary alveolar septa: a possible regulator of ventilation-perfusion ratio? Ultrastructural, immunofluorescence, and in vitro studies. J Cell Biol 60:375–392

Kauffman SL, Burri PH, Weibel ER (1974) The postnatal growth of the rat lung. II. Autoradiography. Anat Rec 180:63–76

Kölliker A (1881) Zur Kenntnis des Baues der Lunge des Menschen. Verh physik-med Ges Würzburg NF 16:1–24

Krogh A, Krogh M (1910) On the rate of diffusion of carbonic oxide into the lungs of man. Skand Arch Physiol 23:236–247

Loring WE, Liebow AA (1954) Effects of bronchial collateral circulation on heart and blood volume. Lab Invest 3:175–196

Low FN (1953) The pulmonary alveolar epithelium of laboratory mammals and man. Anat Rec 117:241–263

Lucocq JM, Mayhew TM, Schwab Y, Steyer AM, Hacker C (2015) Systems biology in 3D space—enter the morphome. Trends Cell Biol 25:59–64

Mason RJ, Shannon JM (1997) Alveolar type II cells. In: Crystal RG, West JB, Weibel ER, Barnes PJ (eds) The lung: scientific foundations, vol 1, 3, 2nd edn. Lippincott Williams & Wilkins, Philadelphia, pp 543–555

Mayhew TM, Lucocq JM (2015) From gross anatomy to the nanomorphome: stereological tools provide a paradigm for advancing research in quantitative morphomics. J Anat 226:309–321

Metcalf DJ, Nightingale TD, Zenner HL, Lui-Roberts WW, Cutler DF (2008) Formation and function of Weibel-Palade bodies. J Cell Sci 121:19–27

Ochs M (2006) A brief update on lung stereology. J Microsc 222:188–200

Ochs M (2010) The closer we look the more we see? Quantitative microscopic analysis of the pulmonary surfactant system. Cell Physiol Biochem 25:27–40

Ochs M, Johnen G, Muller KM, Wahlers T, Hawgood S, Richter J, Brasch F (2002) Intracellular and intraalveolar localization of surfactant protein A (SP-A) in the parenchymal region of the human lung. Am J Respir Cell Mol Biol 26:91–98

Ochs M, Nyengaard JR, Jung A, Knudsen L, Voigt M, Wahlers T, Richter J, Gundersen HJ (2004) The number of alveoli in the human lung. Am J Respir Crit Care Med 169:120–124

Ochs M, Knudsen L, Hegermann J, Wrede C, Grothausmann R, Muhlfeld C (2016) Using electron microscopes to look into the lung. Histochem Cell Biol 146:695–707

Pakkenberg B, Gundersen HJ (1995) Solutions to old problems in the quantitation of the central nervous system. J Neurol Sci 129 Suppl: 65–67

Policard A (1929) Les nouvelles idées sur la disposition de la surface respiratoire pulmonaire. Presse Med 80:1–20

Policard A, Collet A, Pregermain S (1959) Research with the electron microscope on the parietal alveolar cells of the lung of mammals. Z Zellforsch Mikrosk Anat 50:561–587

Ren X, Moser PT, Gilpin SE, Okamoto T, Wu T, Tapias LF, Mercier FE, Xiong L, Ghawi R, Scadden DT, Mathisen DJ, Ott HC (2015) Engineering pulmonary vasculature in decellularized rat and human lungs. Nat Biotechnol 33:1097–1102

Richards DW (1957) Right heart catheterization; its contributions to physiology and medicine. Science 125:1181–1185

Rock JR, Hogan BL (2011) Epithelial progenitor cells in lung development, maintenance, repair, and disease. Annu Rev Cell Dev Biol 27: 493–512

Roughton FJ, Forster RE (1957) Relative importance of diffusion and chemical reaction rates in determining rate of exchange of gases in the human lung, with special reference to true diffusing capacity of pulmonary membrane and volume of blood in the lung capillaries. J Appl Physiol 11:290–302

Sterio DC (1984) The unbiased estimation of number and sizes of arbitrary particles using the disector. J Microsc 134:127–136

Stone KC, Mercer RR, Gehr P, Stockstill B, Crapo JD (1992) Allometric relationships of cell numbers and size in the mammalian lung. Am J Respir Cell Mol Biol 6:235–243

Vanhecke D, Studer D, Ochs M (2007) Stereology meets electron tomography: towards quantitative 3D electron microscopy. J Struct Biol 159:443–450

Vock R, Weibel ER (1993) Massive hemorrhage causes changes in morphometric parameters of lung capillaries and concentration of leukocytes in microvasculature. Exp Lung Res 19:559–577

Wagner DD, Frenette PS (2008) The vessel wall and its interactions. Blood 111:5271–5281

Weibel E (1958) Origination of longitudinal muscles in branches of the bronchial artery. Z Zellforsch Mikrosk Anat 47:440–468

Weibel E (1959) Blood vessel anastomoses in the human lungs. Z Zellforsch Mikrosk Anat 50:653–692

Weibel ER (1963) Morphometry of the human lung. Springer, Berlin

Weibel ER (1970) Morphometric estimation of pulmonary diffusion capacity. I. Model and method. Respir Physiol 11:54–75

Weibel ER (1971) The mystery of "non-nucleated plates" in the alveolar epithelium of the lung explained. Acta Anat (Basel) 78:425–443

Weibel ER (1979) Stereological methods. Academic Press, London

Weibel ER (1984) The pathways of oxygen. Harvard University Press, Cambridge, Mass.

Weibel ER (1991) Fractal geometry: a design principle for living organisms. Am J Physiol 261:L361–L369

Weibel ER (2009) What makes a good lung? Swiss Med Wkly 139:375–386

Weibel ER (2012) Fifty years of Weibel-Palade bodies: the discovery and early history of an enigmatic organelle of endothelial cells. J Thromb Haemost 10:979–984

Weibel ER (2013a) It takes more than cells to make a good lung. Am J Respir Crit Care Med 187:342–346

Weibel ER (2013b) A retrospective of lung morphometry: from 1963 to present. Am J Physiol Lung Cell Mol Physiol 305:L405–L408

Weibel ER (2015) On the tricks alveolar epithelial cells play to make a good lung. Am J Respir Crit Care Med 191:504–513

Weibel ER, Elias H (1967) Quantitative methods in morphology. Springer, Berlin

Weibel ER, Gil J (1968) Electron microscopic demonstration of an extracellular duplex lining layer of alveoli. Respir Physiol 4:42–57

Weibel ER, Gomez DM (1962a) Architecture of the human lung. Use of quantitative methods establishes fundamental relations between size and number of lung structures. Science 137:577–585

Weibel ER, Gomez DM (1962b) A principle for counting tissue structures on random sections. J Appl Physiol 17:343–348

Weibel ER, Knight BW (1964) A morphometric study on the thickness of the pulmonary air-blood barrier. J Cell Biol 21:367–396

Weibel ER, Vidone RA (1961) Fixation of the lung by formalin steam in a controlled state of air inflation. Am Rev Respir Dis 84:856–861

Weibel ER, Federspiel WJ, Fryder-Doffey F, Hsia CC, Konig M, Stalder-Navarro V, Vock R (1993) Morphometric model for pulmonary diffusing capacity. I. Membrane diffusing capacity. Respir Physiol 93:125–149

Weibel ER, Hsia CC, Ochs M (2007) How much is there really? Why stereology is essential in lung morphometry. J Appl Physiol 102: 459–467

Yamaguchi K, Nguyen-Phu D, Scheid P, Piiper J (1985) Kinetics of O2 uptake and release by human erythrocytes studied by a stopped-flow technique. J Appl Physiol 58:1215–1224